Journal of
Mechanics of
Materials and Structures

SOLUTION OF A RECEDING CONTACT PROBLEM USING AN ANALYTICAL METHOD AND A FINITE ELEMENT METHOD

Erdal Öner, Murat Yaylacı and Ahmet Birinci

Volume 9, No. 3

May 2014

msp

JOURNAL OF MECHANICS OF MATERIALS AND STRUCTURES
Vol. 9, No. 3, 2014
dx.doi.org/10.2140/jomms.2014.9.333

SOLUTION OF A RECEDING CONTACT PROBLEM USING AN ANALYTICAL METHOD AND A FINITE ELEMENT METHOD

ERDAL ÖNER, MURAT YAYLACI AND AHMET BİRİNCİ

In this study, a receding contact problem for two elastic layers supported by a Winkler foundation is handled using two different methods such as an analytical method and a finite element method. Firstly, the problem is solved analytically using linear elasticity theory. Then, in order to solve the same problem in a different way, a finite element model of the problem is created by ANSYS software, and finite element analysis of the problem is performed. The contact stresses and the contact areas at the interfaces between punch–Layer 2 and Layer 1–Layer 2 are obtained for both solutions, and it is shown that the finite element method indicates a good agreement with the analytical method.

1. Introduction

Although in the majority of cases the contact zone increases after the application of the load, there are others where the final contact zone is smaller than the original. This type of contact problem is termed as a receding contact problem [Garrido and Lorenzana 1998]. As a different point of view, a receding contact is one where the contact surface in the loaded configuration is contained within the initial contact surface [Johnson 1985]. The studies considering receding contact problems have been performed by various researchers in the literature [Stippes et al. 1962; Wilson and Goree 1967; Weitsman 1969; Margetson and Morland 1970; Chan and Tuba 1971; Keer et al. 1972; Ratwani and Erdogan 1973; Jing and Liao 1990; Porter and Hills 2002]. Furthermore, Zhu [1995] studied a finite element–mathematical programming method for elastoplastic contact problems with friction. Papadopoulos and Solberg [1998] investigated a novel Lagrange multiplier–based formulation for the finite element solution of the quasistatic two-body contact problem in the presence of finite motions and deformations. BEM solution of two-dimensional contact problems by weak application of contact conditions with nonconforming discretizations was carried out by Blázquez et al. [1998]. The mortar finite element method for contact problems was examined by Belgacem et al. [1998]. Guyot et al. [2000] presented coupling of finite elements and boundary elements methods for study of the frictional contact problem. Çömez et al. [2004] solved the plane symmetric double receding contact problem for a rigid stamp and two elastic layers having different elastic constants and heights. A residual type a posteriori error estimator for finite element approximations of a frictional contact problem for linearized elastic materials was analyzed by Bostan and Han [2006]. The plane problem of a frictionless receding contact between an elastic functionally graded layer and a homogeneous half-space when the two bodies were pressed together has been reported by El-Borgi et al. [2006]. Solberg et al. [2007] studied a family of simple two-pass dual formulations for the finite element solution of contact problems. Oysu [2007] investigated finite element and boundary element contact stress analysis with remeshing technique.

Keywords: finite element method, integral equation, receding contact, Winkler foundation.

A frictionless receding contact problem between an anisotropic elastic layer and an anisotropic elastic half-plane, when the two bodies were pressed together by means of a rigid circular stamp, was investigated by Kahya et al. [2007]. Rhimi et al. [2009] extended work of El-Borgi et al. [2006] in the sense that the receding contact problem was solved under axisymmetric conditions rather than plane stress or plane strain conditions. Kuss and Lebon [2009] carried out stress-based finite element methods for solving contact problems and comparisons between various solution methods. Finite element approximation to a contact problem for a nonlinear thermoviscoelastic beam was considered by Copetti and Fernández [2011]. A finite element method used in contact problems with dry friction was investigated by Pop et al. [2011]. Rhimi et al. [2011] focused on a double receding contact axisymmetric problem between a functionally graded layer and a homogeneous substrate. Zhang et al. [2012] reported a finite element model for 2-D elastic–plastic contact analysis of multiple Cosserat materials. Adıbelli et al. [2013] studied receding contact problem for a coated layer and a half-plane loaded by a rigid cylindrical stamp. A numerical approximation by the finite element method of a quasistatic, frictionless, unilateral contact problem between two thermoelastic bodies, in two dimensions, was examined by Copetti [2014]. An axisymmetric Hertzian contact problem of a rigid sphere pressing into an elastic half-space under cyclic loading was investigated by Kim and Jang [2014].

In this paper, a receding contact problem for two elastic layers supported by a Winkler foundation is solved using an analytical method and a finite element method. Thus, it is aimed to see whether FEM results are in an agreement with analytical results and how much the degree of approximation for the two methods is. For this purpose, the problem is firstly solved analytically using linear elasticity theory. Then, a finite element model of the problem is created by ANSYS software, and finite element analysis of the problem is performed. Finally, the contact stresses and the contact areas at the interfaces between punch–Layer 2 and Layer 1–Layer 2 are obtained for both solutions and the results obtained from two different methods are compared with each other.

2. Analytical solution of the problem

Consider the plane strain problem described by the insert in Figure 1, in which the $x = 0$ plane is assumed to be a plane of symmetry. The problem consists of two infinitely long layers of thicknesses h_1 and h_2. The layers are isotropic, homogeneous and linearly elastic. A concentrated load with magnitude P is subjected to the Layer 2 by means of a rigid circular punch. The Layer 1 is supported by a Winkler

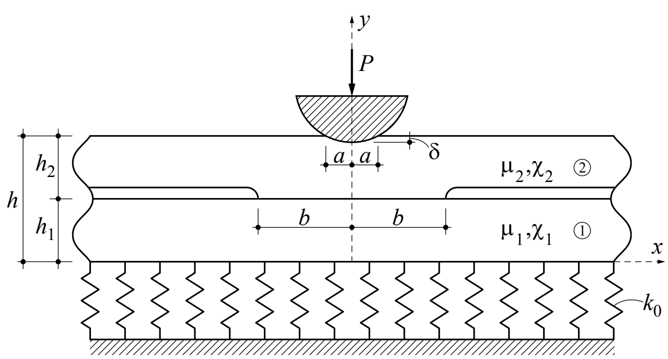

Figure 1. Geometry of the receding contact problem.

foundation. It is assumed that friction and gravity forces are neglected. Since the contact between the two bodies is assumed to be frictionless and layers are not adhered to each other, then only compressive normal tractions can be transmitted in the contact area. Where applicable, the germane quantities are reckoned per unit length in the z direction. Observing that $x = 0$ is a plane symmetry, it is sufficient to consider the problem in the region $0 \le x < \infty$ only.

The stress and the displacement components needed for the application of the boundary conditions can be obtained using linear elasticity theory and integral transform technique as

$$u_i(x, y) = \frac{2}{\pi}\int_0^\infty \{[A_i + B_i y]e^{-\alpha y} + [C_i + D_i y]e^{\alpha y}\}\sin(\alpha x)\,d\alpha, \tag{1}$$

$$v_i(x, y) = \frac{2}{\pi}\int_0^\infty \left\{\left[A_i + B_i\left(\frac{\chi_i}{\alpha} + y\right)\right]e^{-\alpha y} + \left[-C_i + D_i\left(\frac{\chi_i}{\alpha} - y\right)\right]e^{\alpha y}\right\}\cos(\alpha x)\,d\alpha, \tag{2}$$

$$\frac{1}{2\mu_i}\sigma_{x_i}(x, y) = \frac{2}{\pi}\int_0^\infty \left\{\left[\alpha(A_i + B_i y) - \left(\frac{3-\chi_i}{2}\right)B_i\right]e^{-\alpha y} + \left[\alpha(C_i + D_i y) + \left(\frac{3-\chi_i}{2}\right)D_i\right]e^{\alpha y}\right\} \times\cos(\alpha x)\,d\alpha, \tag{3}$$

$$\frac{1}{2\mu_i}\sigma_{y_i}(x, y) = \frac{2}{\pi}\int_0^\infty \left\{-\left[\alpha(A_i + B_i y) + \left(\frac{1+\chi_i}{2}\right)B_i\right]e^{-\alpha y} + \left[-\alpha(C_i + D_i y) + \left(\frac{1+\chi_i}{2}\right)D_i\right]e^{\alpha y}\right\} \times\cos(\alpha x)\,d\alpha, \tag{4}$$

$$\frac{1}{2\mu_i}\tau_{xy_i}(x, y) = \frac{2}{\pi}\int_0^\infty \left\{-\left[\alpha(A_i + B_i y) + \left(\frac{\chi_i-1}{2}\right)B_i\right]e^{-\alpha y} + \left[\alpha(C_i + D_i y) - \left(\frac{\chi_i-1}{2}\right)D_i\right]e^{\alpha y}\right\} \times\sin(\alpha x)\,d\alpha, \tag{5}$$

where $\boldsymbol{u}$ and $\boldsymbol{v}$ are the x and y components of the displacement vector, respectively; σ_x, σ_y and τ_{xy} are the stress components; μ_i is shear modulus; χ_i is an elastic constant and $\chi_i = (3 - 4\nu_i)$ for plane strain; and ν_i is Poisson's ratio $(i = 1, 2)$. The subscripts 1 and 2 refer to Layer 1 and Layer 2, respectively. A_i, B_i, C_i and D_i $(i = 1, 2)$ are the unknown coefficients that will be determined from continuity and boundary conditions prescribed on $y = 0$, $y = h_1$ and $y = h$.

The receding contact problem outlined above as shown in Figure 1 must be solved under the following boundary conditions:

$$\sigma_{y_2}(x, h) = \begin{cases} -p_1(x) & (0 \le x < a), \\ 0 & (a \le x < \infty), \end{cases} \tag{6}$$

$$\tau_{xy_2}(x, h) = 0 \qquad (0 \le x < \infty), \tag{7}$$

$$\sigma_{y_2}(x, h_1) = \begin{cases} -p_2(x) & (0 \le x < b), \\ 0 & (b \le x < \infty), \end{cases} \tag{8}$$

$$\tau_{xy_2}(x, h_1) = 0 \qquad (0 \le x < \infty), \tag{9}$$

$$\sigma_{y_1}(x, h_1) = \sigma_{y_2}(x, h_1) \qquad (0 \le x < \infty), \tag{10}$$

$$\tau_{xy_1}(x, h_1) = 0 \qquad (0 \le x < \infty), \tag{11}$$

$$\tau_{xy_1}(x,0)=0 \qquad (0\le x<\infty), \tag{12}$$

$$\sigma_{y_1}(x,0)=k_0 v_1(x,0) \qquad (0\le x<\infty), \tag{13}$$

$$v_2(x,h)=F(x) \quad \text{or} \quad \frac{\partial}{\partial x}v_2(x,h)=f(x) \qquad (0\le x<a), \tag{14}$$

$$\frac{\partial}{\partial x}[v_2(x,h_1)-v_1(x,h_1)]=0 \qquad (0\le x<b), \tag{15}$$

where a is the half-width of the contact area between rigid circular punch and Layer 2; b is the half-width of the contact area between Layer 1 and Layer 2; $p_1(x)$ is the unknown contact stress under the rigid circular punch; $p_2(x)$ is the unknown contact stress between Layer 1 and Layer 2; k_0 is the stiffness of the Winkler foundation; and $f(x)$ is the derivative of the function $F(x)$ that characterizes surface profile of the rigid punch. In the case of circular punch, $f(x)$ can be written as

$$F(x)=h-\delta-[(R^2-x^2)^{1/2}-R], \tag{16}$$

$$f(x)=\frac{d}{dx}[F(x)]=-\frac{x}{(R^2-x^2)^{1/2}}, \tag{17}$$

where δ is the maximum displacement that occurs on the layer under the punch at the axis of symmetry ($x=0$) and R is the radius of the rigid circular punch. By making use of the boundary conditions (6)–(13), eight of the unknown coefficients A_i, B_i, C_i and D_i ($i=1,2$) appearing in (1)–(5) may be obtained in terms of the unknown functions $p_1(x)$and $p_2(x)$.

By substituting these coefficients into (14) and (15), after some routine manipulations and using the symmetry conditions $p_1(x)=p_1(-x)$ and $p_2(x)=p_2(-x)$ and replacing $\omega=\alpha h$ and $r=h_1/h$, the system of integral equations for $p_1(x)$ and $p_2(x)$ is obtained as

$$\frac{1}{\pi}\int_{-a}^{a}\Big[\frac{1}{t-x}+k_1(x,t)\Big]p_1(t)\,dt+\frac{1}{\pi}\int_{-b}^{b}[k_2(x,t)]p_2(t)\,dt=-\frac{4\mu_2}{(1+\chi_2)}f(x), \tag{18}$$

$$\frac{1}{\pi}\int_{-b}^{b}\Big[\frac{1}{t-x}+k_3(x,t)\Big]p_2(t)\,dt+\frac{1}{\pi}\int_{-a}^{a}[k_4(x,t)]p_1(t)\,dt=0, \tag{19}$$

where

$$k_1(x,t)=\int_0^\infty\Big[\frac{4}{\Delta}K_{11}K_{12}-1\Big]\sin\frac{\omega(t-x)}{h}\,d\omega, \tag{20}$$

$$k_2(x,t)=-8\int_0^\infty\frac{e^{-\omega}e^{-\omega r}}{\Delta}K_{11}K_{13}\sin\frac{\omega(t-x)}{h}\,d\omega, \tag{21}$$

$$k_3(x,t)=\int_0^\infty\Big\{-\frac{4}{(1+m)}\frac{1}{\Delta}\Big\{K_{12}(-K_{11})+mK_{14}\Big[-4\frac{\omega}{h}K_{11A}+K^{**}(1+e^{4\omega r}-2e^{2\omega r})\Big]\Big\}-1\Big\} \times\sin\frac{\omega(t-x)}{h}\,d\omega, \tag{22}$$

$$k_4(x,t)=-\frac{8}{(1+m)}\int_0^\infty\frac{e^{-\omega}e^{-\omega r}}{\Delta}K_{11}K_{13}\sin\frac{\omega(t-x)}{h}\,d\omega, \tag{23}$$

$$\Delta = 4K_{11}K_{14}, \tag{24}$$

$$K_{11} = K^{**}K_{11A} + 4(\omega/h)K_{11B}, \tag{25}$$

$$K_{12} = e^{-4\omega r} - e^{-4\omega} + e^{-2\omega}e^{-2\omega r}(4\omega - 4\omega r), \tag{26}$$

$$K_{13} = e^{-2\omega r}(1+\omega-\omega r) + e^{-2\omega}(-1+\omega-\omega r), \tag{27}$$

$$K_{14} = e^{-4\omega r} + e^{-4\omega} - 2e^{-2\omega}e^{-2\omega r}(1+2\omega^2+2\omega^2 r^2 - 4\omega^2 r), \tag{28}$$

$$K_{11A} = 1 - 4\omega r e^{2\omega r} - e^{4\omega r}, \tag{29}$$

$$K_{11B} = -1 + e^{2\omega r}(2 + 4\omega^2 r^2 - e^{2\omega r}), \tag{30}$$

$$m = \frac{(1+\chi_1)\mu_2}{(1+\chi_2)\mu_1}, \tag{31}$$

$$K^{**} = k(1+\chi_1), \tag{32}$$

$$k = \frac{k_0}{\mu_1}. \tag{33}$$

In the system of singular integral equations (18) and (19), in addition to the contact stresses $p_1(x)$ and $p_2(x)$, the half-width of the contact areas a and b are also unknown. These two unknowns a and b are determined from the equilibrium conditions, which can be written as

$$\int_{-a}^{a} p_1(t)\,dt = P, \qquad \int_{-b}^{b} p_2(t)\,dt = P. \tag{34}$$

We will use (x_1, t_1) to denote the variables (x, t) on the boundary $y = h$, and likewise (x_2, t_2) on the boundary $y = h_1$. We also define the following dimensionless quantities:

$$\begin{gathered} x_1 = ar_1, \quad t_1 = as_1, \quad dt_1 = a\,ds_1, \quad x_2 = br_2, \quad t_2 = bs_2, \quad dt_2 = b\,ds_2, \\ g_1(s_1) = \frac{p_1(t_1)}{P/h}, \quad g_2(s_2) = \frac{p_2(t_2)}{P/h}, \\ M_1(r_1,s_1) = k_1(x_1,t_1), \quad M_2(r_1,s_2) = k_2(x_1,t_2), \quad M_3(r_2,s_2) = k_3(x_2,t_2), \quad M_4(r_2,s_1) = k_4(x_2,t_1). \end{gathered} \tag{35}$$

By substituting (35) into the system of integral equations (18) and (19) and equilibrium conditions (34), the system of integral equations and equilibrium conditions may be obtained as

$$\frac{1}{\pi}\int_{-1}^{1}\Big[\frac{1}{s_1-r_1} + \frac{a}{h}M_1(r_1,s_1)\Big]g_1(s_1)\,ds_1 + \frac{1}{\pi}\frac{b}{h}\int_{-1}^{1} M_2(r_1,s_2)g_2(s_2)\,ds_2 = -\frac{4\mu_2}{(1+\chi_2)P/h}f(r_1), \tag{36}$$

$$\frac{1}{\pi}\int_{-1}^{1}\Big[\frac{1}{s_2-r_2} + \frac{b}{h}M_3(r_2,s_2)\Big]g_2(s_2)\,ds_2 + \frac{1}{\pi}\frac{a}{h}\int_{-1}^{1} M_4(r_2,s_1)g_1(s_1)\,ds_1 = 0, \tag{37}$$

$$\frac{a}{h}\int_{-1}^{1} g_1(s_1)\,ds_1 = 1, \qquad \frac{b}{h}\int_{-1}^{1} g_2(s_2)\,ds_2 = 1. \tag{38}$$

Since (36)–(37) have no closed-form solution, an effective numerical solution may be obtained by using [Erdogan and Gupta 1972]. This method is a standard and necessary step in handling the integral equation part of the solution. So one may notice that because of the smooth contact at the end points a and b, the contact stresses $p_1(x)$ and $p_2(x)$ are zero at the end points, and the index of the integral equations (36) and (37) is "-1". Let

$$g_1(s_1) = G_1(s_1)(1-s_1^2)^{1/2} \quad (-1 < s_1 < 1), \tag{39}$$

$$g_2(s_2) = G_2(s_2)(1-s_2^2)^{1/2} \quad (-1 < s_2 < 1). \tag{40}$$

Using the appropriate Gauss–Chebyshev integration formula, (36)–(38) become

$$\sum_{k=1}^{N} \frac{1-s_k^2}{N+1} \left\{ G_1(s_{k1}) \left[\frac{1}{s_{k1}-r_{i1}} + \frac{a}{h} M_1(r_{i1}, s_{k1}) \right] + \frac{b}{h} M_2(r_{i1}, s_{k2}) G_2(s_{k2}) \right\} = -\frac{4\mu_2}{(1+\chi_2)P/h} f(r_{i1}), \tag{41}$$

$$\sum_{k=1}^{N} \frac{1-s_k^2}{N+1} \left\{ G_2(s_{k2}) \left[\frac{1}{s_{k2}-r_{i2}} + \frac{b}{h} M_3(r_{i2}, s_{k2}) \right] + \frac{a}{h} M_4(r_{i2}, s_{k1}) G_1(s_{k1}) \right\} = 0, \tag{42}$$

$$\frac{a}{h} \sum_{k=1}^{N} \frac{1-s_k^2}{N+1} G_1(s_{k1}) = \frac{1}{\pi}, \qquad \frac{b}{h} \sum_{k=1}^{N} \frac{1-s_k^2}{N+1} G_2(s_{k2}) = \frac{1}{\pi}, \tag{43}$$

where

$$s_k = \cos\left(\frac{k\pi}{N+1}\right) \qquad (k = 1, \ldots, N), \tag{44}$$

$$r_i = \cos\left(\frac{2i-1}{N+1}\frac{\pi}{2}\right) \quad (i = 1, \ldots, N+1). \tag{45}$$

As the value of N is increased, more accurate results can be obtained. Hence, the value of N is chosen as 60 in this study because, after a value of $N = 60$, change in the results is very small and insignificant. It can be seen that the extra equations in (41) and (42) correspond to the consistency condition of the original integral equations (36) and (37). It can also be shown that the $(N/2+1)$-th equations in (41) and (42) are automatically satisfied [Erdogan and Gupta 1972]. Thus, (41)–(43) give $2N+2$ algebraic equations to determine the $2N+2$ unknowns $G_1(s_{k1})$, $G_2(s_{k2})$ $(k = 1, \ldots, N)$, a and b. The system of equations are linear in $G_1(s_{k1})$ and $G_2(s_{k2})$ but highly nonlinear in a and b. Therefore, an interpolation and iteration scheme had to be used to obtain these two unknowns. In this iterative procedure, firstly $2N$ equations $(i = 1, \ldots, N/2, N/2+2, \ldots, N+1)$ are chosen from (41)–(42). After predicting values for a and b, $G_1(s_{k1})$ and $G_2(s_{k2})$ are calculated using previously determined $(2N)$ equations. If the chosen a and b and obtained $G_1(s_{k1})$ and $G_2(s_{k2})$ values ensure (43), the solution would have been found. Otherwise, $G_1(s_{k1})$ and $G_2(s_{k2})$ values are recalculated after predicting new a and b values.

3. The finite-element analysis of the problem

This section describes our FEM analysis of the receding contact problem using ANSYS Multiphysics. The problem is considered as a two-dimensional contact problem, and the material of the layers are assumed elastic and isotropic. The physical system under consideration exhibits symmetry in geometry, material properties and loading. It is computationally advantageous to model only a representative portion. The geometry and the applied load are shown schematically in Figure 2, and the deformed

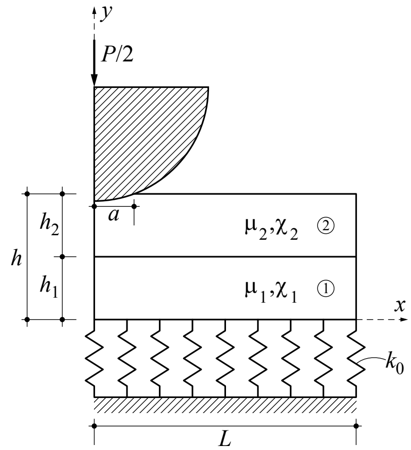

Figure 2. The geometry for the analysis.

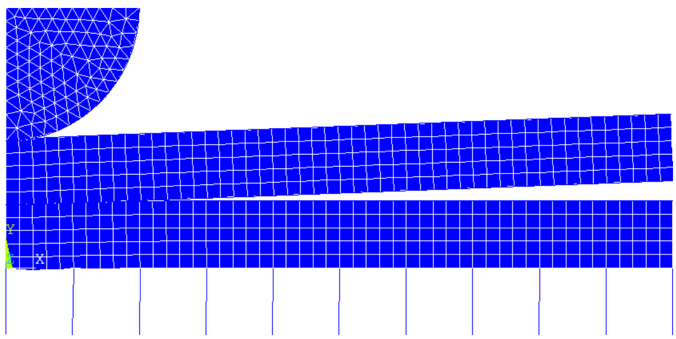

Figure 3. Deformed geometry for the preliminary analysis.

geometry for the preliminary analysis is shown in Figure 3. In the study, two-dimensional solid elements (PLANE183) are used to model the layers. The PLANE183 element is defined by six nodes having two degrees of freedom at each node: translations in the nodal x and y directions. The element may be used as a plane element (plane stress, plane strain and generalized plane strain). The Winkler foundation is modeled by a linear spring element (COMBIN14). The COMBIN14 element or the longitudinal element spring-damper option is an uniaxial tension–compression element with up to two degrees of freedom at each node: translations in the nodal x and y directions. No bending or torsion is considered [Al-Azzawi et al. 2010].

The contact region is meshed by surface-to-surface CONTA172 and TARGE169 contact elements. CONTA172 is used to represent that of the mechanical contact analysis. The target surface, defined by TARGE169, was therefore used to represent 2-D "target" surfaces for the associated contact elements CONTA172. Plane strain finite elements are used for the meshing of the entire geometry. Frictionless surface-to-surface contact elements are used to model the interaction between the contact surfaces, and the augmented Lagrangian method is used as the contact algorithm. The preliminary analysis is meshed with 4435 elements and 8444 nodes, and the contacting line is meshed with 75 elements.

4. Results and discussion

This section presents some of the calculated results obtained from analytical and FEM solution of the receding contact problem for various dimensionless quantities such as R/h, $\mu_2/(P/h)$, μ_2/μ_1 and $k = k_0/\mu_1$. Also, in this section, the results obtained from the analytical method are compared with those of the finite element method.

Table 1 shows variation of half-widths of the contact areas with radius of punch (R/h). It is seen from Table 1 that half-widths of the contact areas increase with increasing radius of punch. This is an expected result. Variation of half-widths of the contact areas with load ratio $\mu_2/(P/h)$ is given in Table 2. Examination of Table 2 indicates that half-widths of the contact areas decrease with increasing of the load ratio $\mu_2/(P/h)$.

Table 3 illustrates the effect of μ_2/μ_1 on the half-widths of the contact areas. As seen in Table 3, increasing the value of μ_2/μ_1 results in an increase of half-widths of the contact areas. Variation of half-widths of the contact areas with $k = k_0/\mu_1$ is presented in Table 4. This table demonstrates that, as the stiffness of the Winkler foundation increases, half-widths of the contact areas decrease. Additionally, when comparing the analytical and FEM results, it is seen from results that the finite element method

Parameter	$R/h = 50$		$R/h = 100$		$R/h = 250$		$R/h = 500$	
	a/h	b/h	a/h	b/h	a/h	b/h	a/h	b/h
Analytical	0.5057	0.7662	0.7079	0.9018	1.0614	1.1882	1.4034	1.4956
FEM	0.500	0.755	0.700	0.900	1.050	1.200	1.400	1.500
Error (%)	1.13	1.15	1.12	0.19	1.07	0.99	0.24	0.29

Table 1. Variation of half-widths of the contact areas with radius of punch (R/h) ($\chi_1 = \chi_2 = 2$, $\mu_2/(P/h) = 100$, $h_1/h = 0.5$, $\mu_2/\mu_1 = 0.5$, $k = k_0/\mu_1 = 2$).

Parameter	$\mu_2/(P/h) = 50$		$\mu_2/(P/h) = 100$		$\mu_2/(P/h) = 200$		$\mu_2/(P/h) = 500$	
	a/h	b/h	a/h	b/h	a/h	b/h	a/h	b/h
Analytical	1.199	1.3707	0.8477	1.0959	0.5735	0.9253	0.3365	0.8236
FEM	1.200	1.375	0.850	1.100	0.575	0.925	0.3375	0.825
Error (%)	0.08	0.31	0.27	0.37	0.25	0.03	0.3	0.17

Table 2. Variation of half-widths of the contact areas with load ratio $\mu_2/(P/h)$ ($\chi_1 = \chi_2 = 2$, $R/h = 100$, $h_1/h = 0.5$, $\mu_2/\mu_1 = 0.5$, $k = k_0/\mu_1 = 0.5$).

Parameter	$\mu_2/\mu_1 = 0.1$		$\mu_2/\mu_1 = 0.5$		$\mu_2/\mu_1 = 2$		$\mu_2/\mu_1 = 5$	
	a/h	b/h	a/h	b/h	a/h	b/h	a/h	b/h
Analytical	0.6013	0.7445	0.7079	0.9018	0.9868	1.2616	1.3112	1.6763
FEM	0.600	0.750	0.700	0.900	0.9875	1.2625	1.3125	1.675
Error (%)	0.22	0.74	1.12	0.19	0.07	0.07	0.1	0.08

Table 3. Variation of half-widths of the contact areas with μ_2/μ_1 ($\chi_1 = \chi_2 = 2$, $\mu_2/(P/h) = 100$, $R/h = 100$, $h_1/h = 0.5$, $k = k_0/\mu_1 = 2$).

Parameter	$k=0.5$		$k=1$		$k=2$		$k=4$	
	a/h	b/h	a/h	b/h	a/h	b/h	a/h	b/h
Analytical	0.8477	1.0959	0.7622	0.9791	0.7079	0.9018	0.6743	0.8528
FEM	0.850	1.100	0.7625	0.975	0.700	0.900	0.675	0.850
Error (%)	0.27	0.37	0.04	0.42	1.12	0.19	0.1	0.33

Table 4. Variation of half-widths of the contact areas with $k = k_0/\mu_1$ ($\chi_1 = \chi_2 = 2$, $\mu_2/(P/h) = 100$, $R/h = 100$, $h_1/h = 0.5$, $\mu_2/\mu_1 = 0.5$).

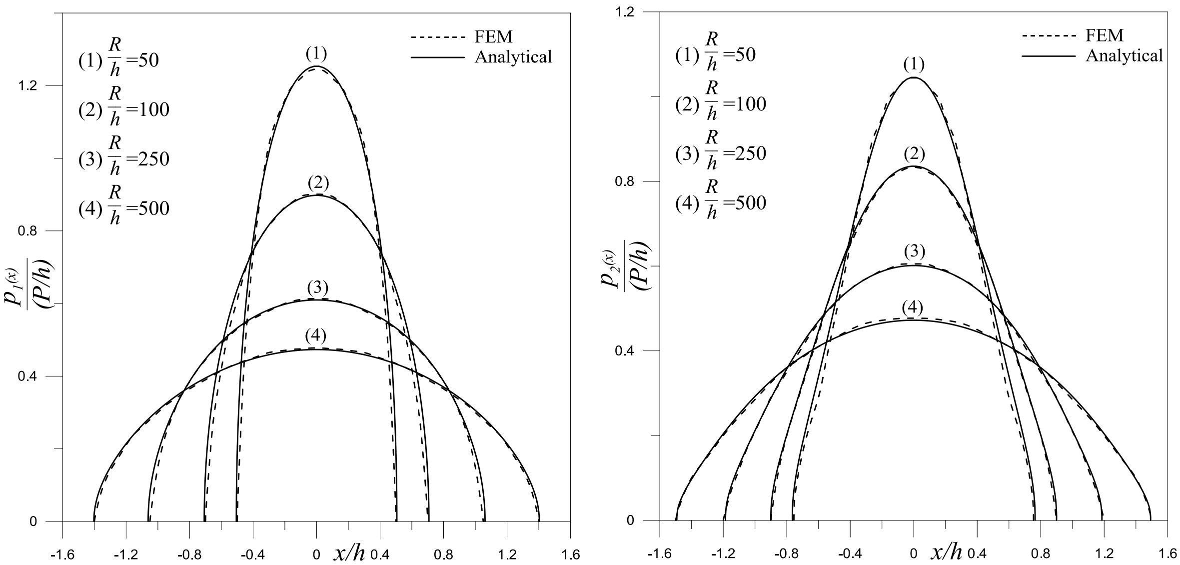

Figure 4. Normalized contact stress distribution at the punch–Layer 2 interface (left) and Layer 1–Layer 2 interface (right) for various values of R/h ($\chi_1 = \chi_2 = 2$, $\mu_2/(P/h) = 100$, $h_1/h = 0.5$, $\mu_2/\mu_1 = 0.5$, $k = 2$).

indicates a good agreement with the analytical method disagree by 0.03%–1.15%. It can be stated that these values are at an acceptable level.

Figure 4 shows normalized contact stress distributions at the interfaces between the rigid punch–Layer 2 and between Layer 1–Layer 2 for various values of R/h. As seen in this figure, the normalized contact stress distributions decrease at both interfaces with increasing of R/h. The effect of the load ratio $\mu_2/(P/h)$ on the normalized contact stress distributions at the interfaces between the rigid punch–Layer 2 and between Layer 1–Layer 2 is presented in Figure 5. It can be concluded from that figure that increasing the value of $\mu_2/(P/h)$ results in an increase of normalized contact stress distributions at both interfaces. The normalized contact stress distributions at the interfaces between the rigid punch–Layer 2 and between Layer 1–Layer 2 for various values of μ_2/μ_1 appear in Figure 6. It is seen there that, as μ_2/μ_1 increases, the normalized contact stress distributions at both interfaces decrease. Figure 7 shows normalized contact stress distributions at the interfaces between the rigid punch–Layer 2 and between Layer 1–Layer 2 for various values of $k = k_0/\mu_1$. They demonstrate that the normalized contact stress distributions at the interfaces between the rigid punch–Layer 2 and between Layer 1–Layer 2 increase

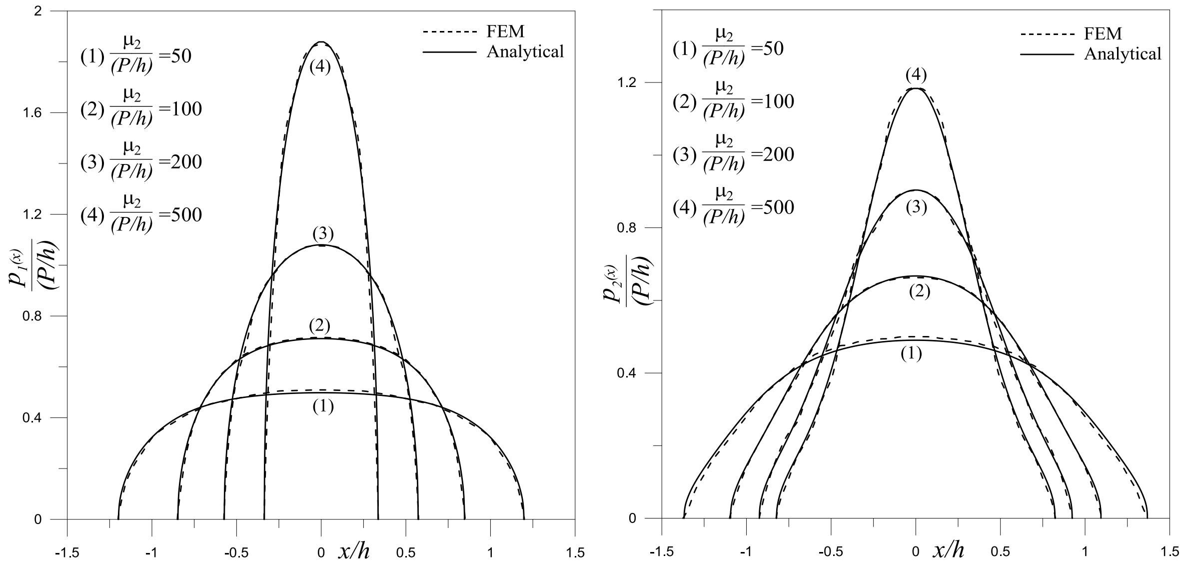

Figure 5. Normalized contact stress distribution at the punch–Layer 2 interface (left) and Layer 1–Layer 2 interface (right) for various values of $\mu_2/(P/h)$ ($\chi_1 = \chi_2 = 2$, $R/h = 100$, $h_1/h = 0.5$, $\mu_2/\mu_1 = 0.5$, $k = 2$).

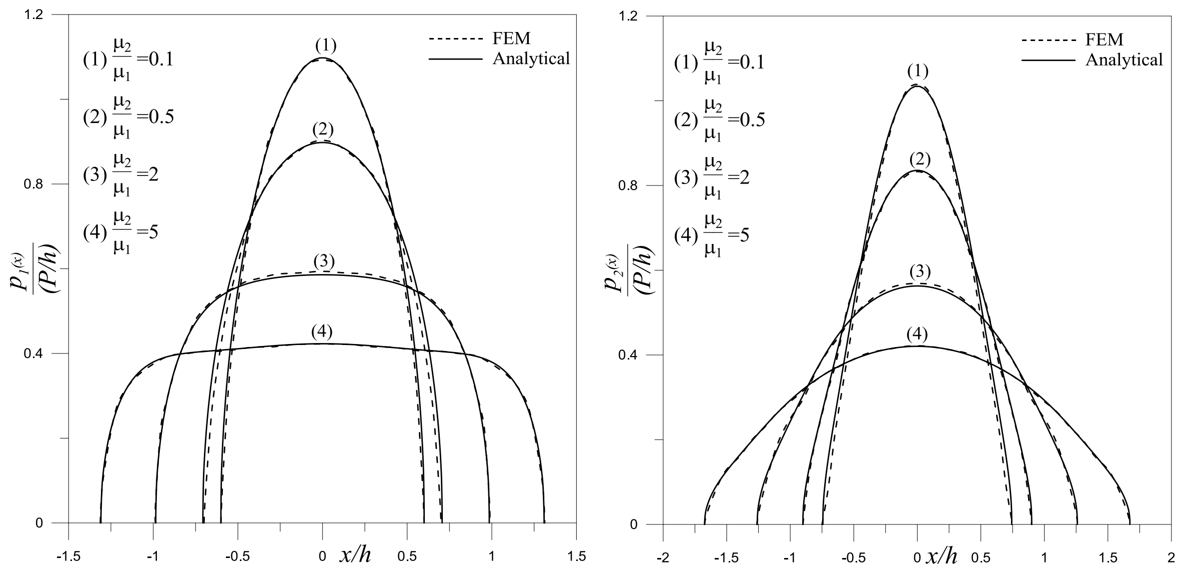

Figure 6. Normalized contact stress distribution at the punch–Layer 2 interface (left) and Layer 1–Layer 2 interface (right) for various values of μ_2/μ_1 ($\chi_1 = \chi_2 = 2$, $R/h = 100$, $\mu_2/(P/h) = 100$, $h_1/h = 0.5$, $k = 2$).

with increasing of the stiffness of the Winkler foundation. All figures show that the normalized contact stress distributions at the interfaces between the rigid punch–Layer 2 and between Layer 1–Layer 2 are symmetrical and their maximum values occur at the axis of symmetry. Also, the values of the

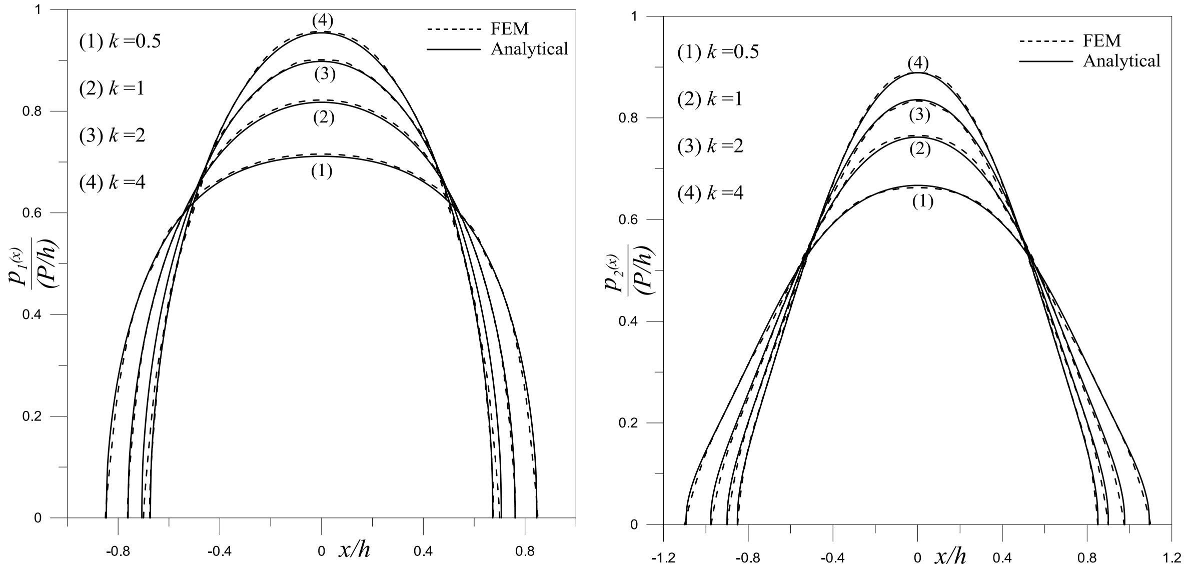

Figure 7. Normalized contact stress distribution at the punch–Layer 2 interface (left) and Layer 1–Layer 2 interface (right) for various values of $k = k_0/\mu_1$ ($\chi_1 = \chi_2 = 2$, $R/h = 100$, $\mu_2/(P/h) = 100$, $h_1/h = 0.5$, $\mu_2/\mu_1 = 0.5$).

normalized contact stresses are zero at the end contact points $(-a, +a)$ and $(-b, +b)$. This result shows that boundary conditions given in the definition of the problem are provided. Finally, similar to results of contact areas, a good agreement is found between the analytical method and FEM.

5. Conclusions

The presented study aims to solve a receding contact problem for two elastic layers supported by a Winkler foundation using two different methods such as an analytical method and a FEM. For this purpose, first of all, the problem is solved analytically using linear elasticity theory. Then, an initial finite element model of the problem is developed by ANSYS software and finite element analysis is performed. Finally, the results obtained from finite element analysis are compared with analytical results. The results of the all analyses described in this paper allow the following conclusions to be drawn:

- Half-widths of the contact areas increase with increasing of R/h and μ_2/μ_1. On the contrary, they decrease with increasing of $\mu_2/(P/h)$ and $k = k_0/\mu_1$.
- Normalized contact stress distributions at the interfaces between the rigid punch–Layer 2 and Layer 1–Layer 2 increase with increasing of $\mu_2/(P/h)$ and $k = k_0/\mu_1$. But increasing the values of R/h and μ_2/μ_1 result in a decrease of normalized contact stress distributions at both interfaces.
- Normalized contact stress distributions at the interfaces between the rigid punch–Layer 2 and between Layer 1–Layer 2 are symmetrical and their maximum values occur at the axis of symmetry. Also, the values of normalized contact stresses are zero at the end contact points $(-a, +a)$ and $(-b, +b)$.

- It is seen from all numerical results that finite element solution indicates a good agreement with analytical solution.

References

[Adıbelli et al. 2013] H. Adıbelli, I. Çömez, and R. Erdöl, "Receding contact problem for a coated layer and a half-plane loaded by a rigid cylindrical stamp", *Arch. Mech.* (*Arch. Mech. Stos.*) **65**:3 (2013), 219–236.

[Al-Azzawi et al. 2010] A. A. Al-Azzawi, A. H. Mahdy, and O. S. Farhan, "Finite element analysis of deep beams on nonlinear elastic foundations", *J. Serbian Soc. Comput. Mech.* **4**:2 (2010), 13–42.

[Belgacem et al. 1998] F. B. Belgacem, P. Hild, and P. Laborde, "The mortar finite element method for contact problems", *Math. Comput. Model.* **28**:4–8 (1998), 263–271.

[Blázquez et al. 1998] A. Blázquez, F. París, and V. Mantič, "BEM solution of two-dimensional contact problems by weak application of contact conditions with non-conforming discretizations", *Int. J. Solids Struct.* **35**:24 (1998), 3259–3278.

[Bostan and Han 2006] V. Bostan and W. Han, "A posteriori error analysis for finite element solutions of a frictional contact problem", *Comput. Methods Appl. Mech. Eng.* **195**:9-12 (2006), 1252–1274.

[Chan and Tuba 1971] S. K. Chan and I. S. Tuba, "A finite element method for contact problems of solid bodies — part I: theory and validation", *Int. J. Mech. Sci.* **13**:7 (1971), 615–625.

[Çömez et al. 2004] I. Çömez, A. Birinci, and R. Erdöl, "Double receding contact problem for a rigid stamp and two elastic layers", *Eur. J. Mech. A Solids* **23**:2 (2004), 301–309.

[Copetti 2014] M. I. M. Copetti, "A penalty-finite element approximation to a Signorini two-body contact problem in thermoelasticity", *Appl. Math. Comput.* **234** (2014), 293–308.

[Copetti and Fernández 2011] M. I. M. Copetti and J. R. Fernández, "Finite element approximation to a contact problem for a nonlinear thermoviscoelastic beam", *J. Math. Anal. Appl.* **383**:2 (2011), 506–521.

[El-Borgi et al. 2006] S. El-Borgi, R. Abdelmoula, and L. Keer, "A receding contact plane problem between a functionally graded layer and a homogeneous substrate", *Int. J. Solids Struct.* **43**:3–4 (2006), 658–674.

[Erdogan and Gupta 1972] F. Erdogan and G. D. Gupta, "On the numerical solution of singular integral equations", *Quart. Appl. Math.* **29** (1972), 525–534.

[Garrido and Lorenzana 1998] J. A. Garrido and A. Lorenzana, "Receding contact problem involving large displacements using the BEM", *Eng. Anal. Bound. Elem.* **21**:4 (1998), 295–303.

[Guyot et al. 2000] N. Guyot, F. Kosior, and G. Maurice, "Coupling of finite elements and boundary elements methods for study of the frictional contact problem", *Comput. Methods Appl. Mech. Eng.* **181**:1–3 (2000), 147–159.

[Jing and Liao 1990] H.-S. Jing and M.-L. Liao, "An improved finite element scheme for elastic contact problems with friction", *Comput. Struct.* **35**:5 (1990), 571–578.

[Johnson 1985] K. L. Johnson (editor), *Contact mechanics*, Cambridge University Press, 1985.

[Kahya et al. 2007] V. Kahya, T. S. Ozsahin, A. Birinci, and R. Erdöl, "A receding contact problem for an anisotropic elastic medium consisting of a layer and a half plane", *Int. J. Solids Struct.* **44**:17 (2007), 5695–5710.

[Keer et al. 1972] L. M. Keer, J. Dundurs, and K. C. Tsai, "Problems involving a receding contact between a layer and a half space", *J. Appl. Mech.* (*ASME*) **39**:4 (12/01 1972), 1115–1120.

[Kim and Jang 2014] J. H. Kim and Y. H. Jang, "Frictional Hertzian contact problems under cyclic loading using static reduction", *Int. J. Solids Struct.* **51**:1 (2014), 252–258.

[Kuss and Lebon 2009] F. Kuss and F. Lebon, "Stress based finite element methods for solving contact problems: comparisons between various solution methods", *Adv. Eng. Software* **40**:8 (2009), 697–706.

[Margetson and Morland 1970] J. Margetson and L. W. Morland, "Separation of smooth circular inclusions from elastic and viscoelastic plates subjected to uniaxial tension", *J. Mech. Phys. Solids* **18**:4 (1970), 295–309.

[Oysu 2007] C. Oysu, "Finite element and boundary element contact stress analysis with remeshing technique", *Appl. Math. Model.* **31**:12 (2007), 2744–2753.

[Papadopoulos and Solberg 1998] P. Papadopoulos and J. M. Solberg, "A Lagrange multiplier method for the finite element solution of frictionless contact problems", *Math. Comput. Model.* **28**:4–8 (1998), 373–384. Recent Advances in Contact Mechanics.

[Pop et al. 2011] N. Pop, H. Cioban, and A. Horvat-Marc, "Finite element method used in contact problems with dry friction", *Comput. Mater. Sci.* **50**:4 (2011), 1283–1285.

[Porter and Hills 2002] M. I. Porter and D. A. Hills, "Note on the complete contact between a flat rigid punch and an elastic layer attached to a dissimilar substrate", *Int. J. Mech. Sci.* **44**:3 (2002), 509–520.

[Ratwani and Erdogan 1973] M. Ratwani and F. Erdogan, "On the plane contact problem for a frictionless elastic layer", *Int. J. Solids Struct.* **9**:8 (1973), 921–936.

[Rhimi et al. 2009] M. Rhimi, S. El-Borgi, W. B. Saïd, and F. B. Jemaa, "A receding contact axisymmetric problem between a functionally graded layer and a homogeneous substrate", *Int. J. Solids Struct.* **46**:20 (2009), 3633–3642.

[Rhimi et al. 2011] M. Rhimi, S. El-Borgi, and N. Lajnef, "A double receding contact axisymmetric problem between a functionally graded layer and a homogeneous substrate", *Mech. Mater.* **43**:12 (2011), 787–798.

[Solberg et al. 2007] J. M. Solberg, R. E. Jones, and P. Papadopoulos, "A family of simple two-pass dual formulations for the finite element solution of contact problems", *Comput. Methods Appl. Mech. Eng.* **196**:4–6 (2007), 782–802.

[Stippes et al. 1962] M. Stippes, H. B. Wilson, Jr., and F. N. Krull, "A contact stress problem for a smooth disk in an infinite plate", pp. 799–806 in *Proceedings of the Fourth U.S. National Congress of Applied Mechanics* (Berkeley, 1962), vol. 2, Amer. Soc. Mech. Engrs., New York, 1962.

[Weitsman 1969] Y. Weitsman, "On the unbonded contact between plates and an elastic half space", *J. Appl. Mech.* (*ASME*) **36**:2 (06/01 1969), 198–202.

[Wilson and Goree 1967] H. B. Wilson, Jr. and J. G. Goree, "Axisymmetric contact stresses about a smooth elastic sphere in an infinite solid stressed uniformly at infinity", *J. Appl. Mech.* (*ASME*) **34**:4 (12/01 1967), 960–966.

[Zhang et al. 2012] H. W. Zhang, Z. Q. Xie, B. S. Chen, and H. L. Xing, "A finite element model for 2D elastic-plastic contact analysis of multiple Cosserat materials", *Eur. J. Mech. A Solids* **31** (2012), 139–151.

[Zhu 1995] C. Zhu, "A finite element-mathematical programming method for elastoplastic contact problems with friction", *Finite Elem. Anal. Des.* **20**:4 (1995), 273–282.

Received 6 Mar 2014. Revised 21 Jul 2014. Accepted 3 Aug 2014.

ERDAL ÖNER: eoner@bayburt.edu.tr
Department of Civil Engineering, Bayburt University, 69000 Bayburt, Turkey

MURAT YAYLACI: murat.yaylaci@erdogan.edu.tr
Department of Civil Engineering, Recep Tayyip Erdoğan University, 53100 Rize, Turkey

AHMET BİRİNCİ: birinci@ktu.edu.tr
Department of Civil Engineering, Karadeniz Technical University, 61080 Trabzon, Turkey

mathematical sciences publishers msp

JOURNAL OF MECHANICS OF MATERIALS AND STRUCTURES

msp.org/jomms

Founded by Charles R. Steele and Marie-Louise Steele

See msp.org/jomms for submission guidelines.

JoMMS (ISSN 1559-3959) at Mathematical Sciences Publishers, 798 Evans Hall #6840, c/o University of California, Berkeley, CA 94720-3840, is published in 10 issues a year. The subscription price for 2014 is US $555/year for the electronic version, and $710/year (+$60, if shipping outside the US) for print and electronic. Subscriptions, requests for back issues, and changes of address should be sent to MSP.

JoMMS peer-review and production is managed by EditFlow® from Mathematical Sciences Publishers.

PUBLISHED BY

mathematical sciences publishers

nonprofit scientific publishing

http://msp.org/

Journal of Mechanics of Materials and Structures

Volume 9, No. 3 May 2014

1559-3959(2014)9:3;1-7